Al-Ali, Ismail, Zweiri, Yahya, Al Moosa, Nawaf, Taha, Tarek, Dias, Jorge and Senevirtane, Lakmal (2019) State of the art in tilt-quadrotors, modelling, control, and fault recovery. Journal of Mechanical Engineering Science - Part C, 234(2), pp. 474-486. Copyright © 2019 ((Sage) DOI: https://doi.org/10.1177%2F0954406219878741.

():1–11

# State of the art in tilt-quadrotors, modelling, control, and fault recovery

Ismail Al-Ali[1]*, Yahya Zweiri[2,1], Nawaf Al Moosa[1], Tarek Taha[1], Jorge Dias[1] and Lakmal Senevirtane[1]


## Abstract

Research studies on quadrotors have recently drawn significant interest from academia and industry. Faults and failures handling are the major weaknesses of conventional quadrotor platforms, therefore an innovative actuation mechanism was introduced to allow tilting the rotors. Tilting rotors of multirotor platforms provide high dexterity for flying between adjacent obstacles and assists the platforms in dealing with various failure scenarios. This paper reviews the state of the research on tilt-quadrotor platforms. Several platforms, software and hardware architectures were discussed in the literature. Most of the latest developments were focused on conventional quadrotor modelling, combined with rotor tilting dynamics. On the other hand, controlling such platform was mainly studied using two types of controllers: Feedback Linearisation technique, and Control Allocator. Recovery strategy in case of fault or failure has been covered extensively for conventional quadrotors, but very limited known work for tilt-quadrotor. This review concludes that the system dynamic modelling is relatively well covered compared to exploring new control techniques for more stringent requirements. However, recovery strategies as the main advantage of tilt-quadrotor platforms are not explored extensively and require more research attention.



## Keywords

Tilt rotors; quadrotor; fault detection and tolerance; recovery strategy; identification; modelling; control


## Introduction

Quadrotors have attracted high level of attention in the industry as well as among research communities since early 1900s. During World War I (WWI), there was a military requirement to develop an aircraft capable of performing Vertical Takeoff and Landing (VTOL). This resulted in two main projects driven by Oehmichen in France,[1] and a less successful project by Bothezat in US.[2] The overall design of the two aircraft looks very similar to quadrotor platform, with large propellers were used to generate sufficient lift, and smaller propellers to perform the manoeuvres. In 1966, the Department of Defence sponsored the development of Bell X-22A large scale aircraft developed by Bell Aerosystems.[3] In 1967, Curtiss-Wright Corporation attempted to develop the X-19, which is a large scale aircraft with capability of performing short vertical takeoff and landing (SVTOL) by tilting its rotors to transition between vertical takeoff and landing, and cruise.[4] All quadrotor projects at that time were called off and no quadrotor system was completed.[5]

In the past two decades, such flying concept was become possible by overcoming the difficulties faced by the older attempts. Some of the main advances allowed development of such flying concept in small scale are the stability augmentation, advances in brushless DC motors, sensors, on-board processors, and batteries. The sensors accuracy and weight are much better compared to old sensors. Also, on-board electronic processing became possible, with low power consumption to execute computationally-heavy stability algorithms. Furthermore, brushless motors became much more reliable, less noisy and very efficient compared to brushed motors. Finally, the amount of electrical charge storage in batteries increased significantly with advances in Lithium Polymer based and Lithium-Ion based batteries.

Conventional quadrotor and tilt-quadrotor platforms are aircraft capable of performing vertical takeoff and landing. The rotors axis of rotation for conventional quadrotor is perpendicular to the aircraft horizontal frame, while the tilt-quadrotor has the capability of tilting the rotor on one axis (single-tilt), or on two axes (dual-tilt). The flying concept is capable of manoeuvring by producing different thrust between rotors to produce rotational moment. Also for tilt-quadrotor, linear motion is possible by orienting the thrust vector of each individual rotor. The overall design is much simpler mechanically compared to conventional helicopters, and is a much more suitable platforms for indoor and urban applications.

Tilt-quadrotor platforms were developed as a concept after development of quadrotors. Conventional quadrotors suffer from a major problem in flight safety. In fact, the platform is under-actuated, thus preventing simultaneous control of all 6-DoF. The conventional quadrotor is capable of controlling only three position variables, and heading.


[1]Khalifa University Center for Autonomous Robotic Systems (KUCARS), Khalifa University of Science and Technology, P.O. Box 127788, Abu Dhabi, UAE
[2]Faculty of Science, Engineering and Computing, Kingston University London, London SW15 3DW, UK

**Corresponding author:**
Ismail Al-Ali, Khalifa University Center for Autonomous Robotic Systems (KUCARS), Khalifa University of Science and Technology, P.O. Box 127788, Abu Dhabi, UAE.
Email: ismail.alali@ku.ac.ae

The attitude is not free to control while maintaining fixed position. Furthermore, a single failure in one rotor may result in a system crash.

Some attempts were made to overcome the failure cases of single rotor by introducing extra set of rotors. This resulted in hexarotor platforms (six rotors), and octarotor platforms (eight rotors). This solution is valid to overcome system crash in case of single motor failure. However, the rotors are still constrained to the horizontal plane (the platform is still under-actuated).

The novel design of quadrotors with tilting mechanism is capable of overcoming the above mentioned problems, including proper recovery from failures. Recovery from failures can be achieved by this design concept through reconfiguration of the over-actuated system. The new concept is capable of performing 6-DoF control were attitude and position are controlled independently. Also, the new concept has better performance in navigating indoor areas since translational forces are produced by tilting the individual thrust vectors. All these advantages make the tilt-quadrotor platforms very attractive for fault and failure recovery.

## Literature Review

### *Platform Development*

Several research groups worked on designing and building the novel actuation of tilt-quadrotors. This resulted in a range of developed platforms driven by different requirements. Some of these platforms have single tilt axis, while few have dual axes tilting rotor.

**Figure 1.** Dual tilt-quadrotor photo.[6]

The platform shown in Figure 1 is developed by coauthor.[6,7] It is a relatively large platform compared to the rest of the platforms in literature. This platform has a mass of 4kg, with 2kg payload capacity. The size and mass of this platform required 2-bladed carbon fibre propellers of size $15 \times 5$ inches. The tilting capability is achieved by two servos; one for the push-pull mechanism, and another servo to rotate the arm.

The software and hardware architecture is discussed by Markus[8] to implement the feedback linearisation based control system.[9] The feasibility of the platform with reasonable capabilities were discussed, and a list of requirements was driven for the avionics, the platform is shown in Figure 2. The list includes the required measurements such as: linear position and velocities (from visual tracking system), angular velocities (from gyroscopes), tilt angle and spinning velocity of rotors (motor controller and servo motor), and linear and angular accelerations. The presented hardware was discussed, which runs a real-time version of Ubuntu operating system.

**Figure 2.** Tilt-quadrotor from[8]

Another work group [10] also developed a platform with different capabilities, as shown in Figure 3. The developed platform has a single tilt axis with 1.4kg weight. The design was driven by the requirement to have a system capable of performing perpendicular hover. Therefore, the tilt mechanism was design to have a wide angle, ranging from 0° to 260°. The platform have thrust to weight ratio of 1.75, and runs a microcomputer RX62T from Renesas Technology.

**Figure 3.** Single Tilt-quadrotor platform photo.[10]

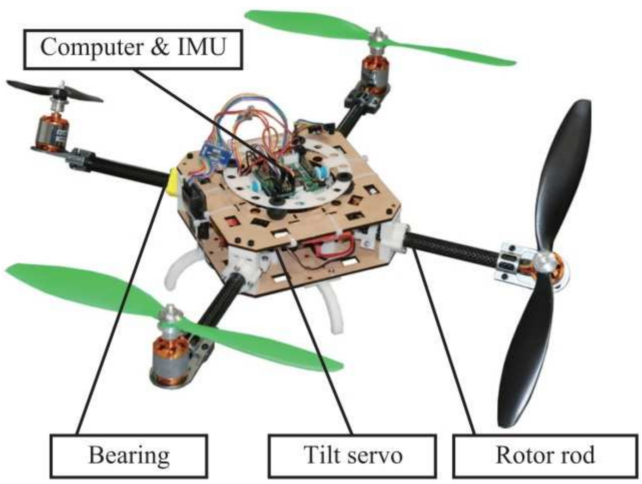


A dual tilt-quadrotor platform[11,12] was developed to have a platform with increased agility and reliability. The design was based on fusing three actuation mechanism, these are: gyroscopic torques, thrust vectoring, and differential thrusting. The resulted platform is illustrated in Figure 4. The avionics of the platform consisted of two power systems: one battery to power the servos, and another battery to power the motors. The avionics make use of already available Commercial Of-the-Shelf Solution (COTS), such as: chipKit Max32 for the processing board, RC servos and motors, and COTS Inertial Navigation System.

**Figure 4.** Dual tilt-quadrotor platform photo.[13]

As one of the main advantages of tilt-quadrotor is the capability of maintaining normal flight operation in failure case, the thrust-to-weight ratio requirement is crucial in the early stages of the platform design. The design of the platform must consider the failure cases and make it feasible to continue the operation of the system in sever failure cases.

## *System Modelling*

*Overview* For the majority of control systems types, a dynamical model is usually required to first simulate the platform, then to design and implement the developed controllers in simulation environment. In this section, the dynamic modelling in the literature is summarised.

**Figure 5.** Overview of the system Model

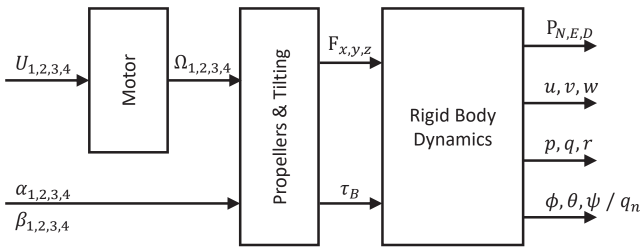


The general structure of the dual tilt-quadrotor system model is illustrated in Figure 5. The high level system model has three inputs; motor PWM commands $U_{1,2,3,4}$, and the two tilt angles $\alpha_{1,2,3,4}$ and $\beta_{1,2,3,4}$. The model is composed of three models, these are: motor model, propeller and tilt model, and rigid body dynamics.

The model describes the motor response to an input command, and produces a set of four motors' angular velocities. The propeller and tilt model in turn takes the motors' angular velocity to produce individual thrust and differential moments. The individual thrust vector is oriented according to the tilt angle inputs. Furthermore, this model includes the tilt mechanism dynamics. Finally, the total forces and moments are fed to a generic rigid body dynamic model which models the rotation and translation dynamics of the platform in 3D space.

**Table 1.** List of symbols

| Variable | Definition | Unit |
|---|---|---|
| $A$ | Rotor disk area, $\pi R^2$ | $m^2$ |
| $C_{l_\alpha}$ | 2-D lift-curve slope of the blade's airfoil | 1 |
| $c$ | Blade chord length | $m$ |
| $\boldsymbol{\mathcal{F}^b}$ | Body FoR, with bases $[\tilde{i}^b, \tilde{j}^b, \tilde{k}^b]$ | |
| $\boldsymbol{\mathcal{F}^{r_i}}$ | $i$-th Rotor FoR, with bases $[\tilde{i}^{r_i}, \tilde{j}^{r_i}, \tilde{k}^{r_i}]$ | |
| $\boldsymbol{\mathcal{F}^w}$ | World Frame of Reference (FoR), with bases $[\tilde{i}^w, \tilde{j}^w, \tilde{k}^w]$ | |
| $F_{x,y,z}$ | Forces on $\boldsymbol{\mathcal{F}^b}$ | $N$ |
| $\boldsymbol{f_i}$ | Force vector of $i$-th rotor on $\boldsymbol{\mathcal{F}^{r_i}}$ FoR | $N$ |
| $N_b$ | Number of rotor blades | 1 |
| $P_{N,E,D}$ | North, East, and Down position of system on $\boldsymbol{\mathcal{F}^w}$ FoR | $m$ |
| $\boldsymbol{P_i^r}$ | Position of $i$-th rotor on $\boldsymbol{\mathcal{F}^b}$ | $m$ |
| $T_h$ | Hover thrust per individual rotor | $N$ |
| $U_i$ | Motor Pulse Width Modulation (PWM) command. $(i = 1, 2, 3, 4)$ | $\mu s$ |
| $u, v, w$ | Forward, side, and down velocities on $\boldsymbol{\mathcal{F}^b}$ FoR | $m/s$ |
| $u_r, v_r, w_r$ | Forward, side, and down relative air velocities on $\boldsymbol{\mathcal{F}^b}$ FoR | $m/s$ |
| $V_x, V_y, V_z$ | Horizontal velocities $V_x, V_y$, and climb velocity on $\boldsymbol{\mathcal{F}^{r_i}}$ velocity | $m/s$ |
| $v_h$ | Rotor induced inflow velocity in hover | $m/s$ |
| $v_i$ | Induced inflow velocity of $i$-th rotor | $m/s$ |
| $\boldsymbol{W^w}$ | North, East, and Down wind velocities $\boldsymbol{\mathcal{F}^w}$ FoR | $m/s$ |
| $\alpha_i$ | Tilt angle of $i$-th rotor around $\tilde{i}^r$ on $\boldsymbol{\mathcal{F}^{r_i}}$ FoR | $rad$ |
| $\beta_i$ | Tilt angle of $i$-th rotor around $\tilde{j}^r$ on $\boldsymbol{\mathcal{F}^{r_i}}$ FoR | $rad$ |
| $\theta_0$ | Blade pitch angle at the root | $rad$ |
| $\theta_{tw}$ | Linear blade twist rate | $rad$ |
| $\kappa$ | Induced power factor | 1 |
| $\lambda_i$ | Induced inflow ratio of $i$-th rotor | 1 |
| $\sigma$ | Rotors' solidty coefficient | 1 |
| $\boldsymbol{\tau_B}$ | Moments on $\boldsymbol{\mathcal{F}^b}$, with elements $[L \quad M \quad N]$ | $N.m$ |
| $\boldsymbol{\tau_i}$ | Moment vector of $i$-th rotor on $\boldsymbol{\mathcal{F}^{r_i}}$ FoR | $N.m$ |
| $\phi, \theta, \psi$ | Roll, pitch, and yaw angles with respect to $\boldsymbol{\mathcal{F}^w}$ FoR. | $rad$ |
| $\Omega_i$ | Angular velocity of the $i$-th rotor around $\tilde{k}^{r_i}$ on $\boldsymbol{\mathcal{F}^{r_i}}$ FoR | $rad/s$ |
| $\boldsymbol{\omega}$ | Body angular velocity vector on $\boldsymbol{\mathcal{F}^b}$ FoR with elements $[p \quad q \quad r]$. | $rad/s$ |
| $\boldsymbol{\omega_{pi}}$ | Angular velocity of the $i$-th rotor on $\boldsymbol{\mathcal{F}^{r_i}}$ FoR with elements $[\dot{\alpha}_i \quad \dot{\beta}_i \quad \Omega_i]^T$ | $rad/s$ |

*Kinematics* As shown in Figure 6, there are three axes. These axes are; World axis $\boldsymbol{\mathcal{F}^w}$, a Body axis indicated by $\boldsymbol{\mathcal{F}^b}$ FoR, and an axis system per each rotor indicated by $\boldsymbol{\mathcal{F}^{r_i}}$

FoR. The body FoR is attached to the system body, moves and rotates with the body.

**Figure 6.** Axis system definition

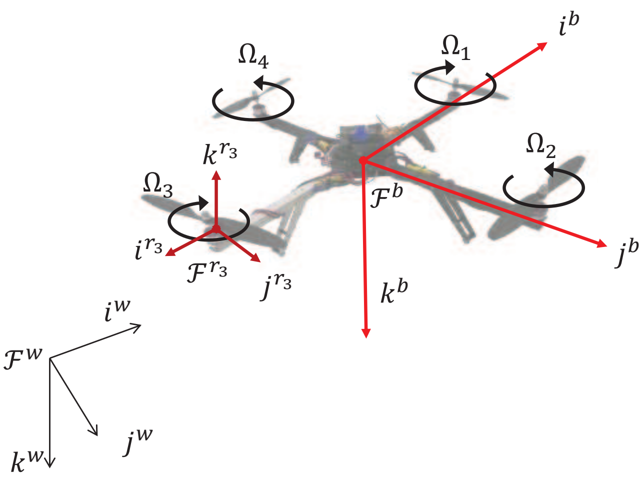


The relationship between position time derivative in $\boldsymbol{\mathcal{F}^w}$ (velocities in world FoR) and body velocities are expressed using the relation in (Eq. 1)

$$\begin{bmatrix} \dot{P}_N \\ \dot{P}_E \\ \dot{P}_D \end{bmatrix} = \boldsymbol{\mathcal{R}^{bw}} \begin{bmatrix} u \\ v \\ w \end{bmatrix} \tag{1}$$

where $\boldsymbol{R^{bw}}$ is Euler Rotation matrix to transforms the projection of a vector from $\boldsymbol{\mathcal{F}^b}$ to $\boldsymbol{\mathcal{F}^w}$. This matrix is defined through three rotations around the axes $\tilde{i}^w$, $\tilde{j}^w$, and $\tilde{k}^w$, respectively.

$$\boldsymbol{\mathcal{R}^{bw}} = \begin{bmatrix} C_\theta C_\psi & S_\phi S_\theta C_\psi - C_\phi S_\psi & C_\phi S_\theta C_\psi + S_\phi S_\psi \\ C_\theta S_\psi & S_\phi S_\theta S_\psi + C_\phi C_\psi & C_\phi S_\theta S_\psi - S_\phi C_\psi \\ -S_\theta & S_\phi C_\theta & C_\phi C_\theta \end{bmatrix} \tag{2}$$

where $C_\alpha = \cos(\alpha)$, $S_\alpha = \sin(\alpha)$.

With the definition of $\boldsymbol{R^{bw}}$ in (Eq. 2), the dynamics of Euler angles ($\phi$, $\theta$, $\psi$) are as follows:

$$\begin{bmatrix} \dot{\phi} \\ \dot{\theta} \\ \dot{\psi} \end{bmatrix} = \begin{bmatrix} 1 & \sin(\phi)\tan(\theta) & \cos(\phi)\tan(\theta) \\ 0 & \cos(\phi) & -\sin(\phi) \\ 0 & \sin(\phi)\sec(\theta) & \cos(\phi)\sec(\theta) \end{bmatrix} \begin{bmatrix} p \\ q \\ r \end{bmatrix} \tag{3}$$

This definition of body rotation in 3D space is very common and used for most flying platforms, including fixed wings and helicopters. Even though this definition is very popular, it is not defined at $\theta = \frac{\pi}{2}$. Conventional fixed wings and helicopters are not concerned with this limitation since this condition is very far from normal operating points. However, systems such as satellites, rockets/missiles, and tilt-quadrotors can operate near $\theta = \frac{\pi}{2}$ for extended period of time.

One possible approach to avoid the singularity is to use Quaternion rotations.[14] Quaternion rotation consists of a vector part, defined in (Eq. 4), and a scalar $e_0$ defined in (Eq. 5).

$$e = e_1\tilde{i}^w + e_2\tilde{j}^w + e_3\tilde{k}^w \tag{4}$$

$$e_0 = \cos\left(\frac{\Phi}{2}\right) \tag{5}$$

The full vector that defines the system attitude in this case is:

$$e = \begin{bmatrix} e_0 & e_1 & e_2 & e_3 \end{bmatrix}^T \tag{6}$$

and the elements propagates over time according to (Eq. 7):

$$\begin{bmatrix} \dot{e}_0 \\ \dot{e}_1 \\ \dot{e}_2 \\ \dot{e}_3 \end{bmatrix} = \frac{1}{2} \begin{bmatrix} 0 & -p & -q & -r \\ p & 0 & r & -q \\ q & -r & 0 & p \\ r & q & -p & 0 \end{bmatrix} \begin{bmatrix} e_0 \\ e_1 \\ e_2 \\ e_3 \end{bmatrix} - \lambda \frac{\partial J}{\partial e} \tag{7}$$

The last term in (Eq. 7) is added to maintain $||e|| = 1$ through careful selection of $\lambda$. The dynamics equation in (Eq. 7) for quaternion rotation replaces Euler rotation dynamics in equation (Eq. 3). Apart from the singularity case, solving via quaternion rotation, makes computation of the dynamics equation (Eq. 7) less expensive.

It is possible to use Euler angles for the rigid body dynamics while the rotation dynamics uses quaternion definition. This can be achieved by transforming between Euler and quaternion definitions using the transformations (Eq. 8-Eq. 14).

$$\phi = \arctan\left(\frac{2(e_0e_1 + e_2e_3)}{e_0^2 + e_3^2 - e_1^2 - e_2^2}\right) \tag{8}$$

$$\theta = \arcsin\left(2(e_0e_2 - e_1e_3)\right) \tag{9}$$

$$\psi = \arctan\left(\frac{2(e_0e_3 + e_1e_2)}{e_0^2 + e_1^2 - e_2^2 - e_3^2}\right) \tag{10}$$

$$e_0 = C_{\frac{\psi}{2}}C_{\frac{\theta}{2}}C_{\frac{\phi}{2}} + S_{\frac{\psi}{2}}S_{\frac{\theta}{2}}S_{\frac{\phi}{2}} \tag{11}$$

$$e_1 = C_{\frac{\psi}{2}}C_{\frac{\theta}{2}}S_{\frac{\phi}{2}} - S_{\frac{\psi}{2}}S_{\frac{\theta}{2}}C_{\frac{\phi}{2}} \tag{12}$$

$$e_2 = C_{\frac{\psi}{2}}S_{\frac{\theta}{2}}C_{\frac{\phi}{2}} + S_{\frac{\psi}{2}}C_{\frac{\theta}{2}}S_{\frac{\phi}{2}} \tag{13}$$

$$e_3 = S_{\frac{\psi}{2}}C_{\frac{\theta}{2}}C_{\frac{\phi}{2}} - C_{\frac{\psi}{2}}S_{\frac{\theta}{2}}S_{\frac{\phi}{2}} \tag{14}$$

*Rigid Body Dynamics* FoR of the rotor is at its centre, moves with the rotor and rotates with respect to body only (no rotation with the rotor blades).

From this definition and the variables indicated in Table 1, the linear motion of the system can be modelled as follows:

$$m\ddot{\boldsymbol{P}} = m\begin{bmatrix} 0 \\ 0 \\ -g \end{bmatrix} + \boldsymbol{R^{bw}} \sum_{i=1}^{4} \left(\boldsymbol{R^{r_ib}} \boldsymbol{f_i}\right) \tag{15}$$

The model in equation (Eq. 15) consists of only two external forces, these are; force due to gravity (first term), and the sum of forces produced by the spinning rotors ($\boldsymbol{f_i}$).

The rotational dynamics of the system is modelled as in equation (Eq. 16).[9] The dynamics of rotation covers the gyroscopic effect due to: system rotation in space, moments $\boldsymbol{\tau_{P_i}}$ produced by rotors, and moments $\boldsymbol{\tau_B}$ produced by differential thrust. The moment due to differential thrust is modelled in $\boldsymbol{\mathcal{F}^{r_i}}$, which is transformed into $\boldsymbol{\mathcal{F}^b}$ using $\boldsymbol{R^{rb}}$, (Eq. 17).

$$\boldsymbol{I_b}\dot{\boldsymbol{\omega}} = \boldsymbol{\tau_B} - \boldsymbol{\omega} \times \boldsymbol{I_b}\boldsymbol{\omega} - \sum_{i=1}^{4} \left(\boldsymbol{R^{r_i b}}\boldsymbol{\tau_{P_i}}\right) \quad (16)$$

$$\boldsymbol{\tau_B} = \begin{bmatrix} L \\ M \\ N \end{bmatrix} = \sum_{i=1}^{4} \left(\boldsymbol{P_i^r} \times \boldsymbol{R^{r_i b}}\boldsymbol{f_i}\right) \quad (17)$$

The moments produce by the rotor is given as:

$$\boldsymbol{\tau_{P_i}} = \boldsymbol{I_{P_i}}\dot{\boldsymbol{\omega}}_{\boldsymbol{pi}} + \boldsymbol{\omega_{pi}} \times \boldsymbol{I_{P_i}}\boldsymbol{\omega_{pi}} + \boldsymbol{\tau_i} \quad (18)$$

*Propellers and Tilting Model* The inputs to the rotor subsystem are motor angular velocity command, and tilt angle. The produced outputs of this subsystem are the forces and moments in $\boldsymbol{\mathcal{F}^b}$, which get transformed into $\boldsymbol{\mathcal{F}^{r_i}}$. In the literature,[11] this subsystem is modelled separately and its output is fed to the Rigid Body dynamic model. The tilting mechanism can be characterised in frequency domain.[11]

There are two models considered in this review for the forces and moments produced by a rotor. The simplest model is a linear mapping of the $i$-th rotor squared angular velocity with produced force and drag moment on rotor's vertical axis $\tilde{k}^{r_i}$, shown in (Eq. 19) and (Eq. 20). The parameters $C_T$ and $C_Q$ are the rotor's thrust coefficient and drag coefficient, respectively. These parameters can be obtained experimentally.

$$\boldsymbol{f_i} = C_T\Omega_i^2\tilde{k}^{r_i} \quad (19)$$

$$\boldsymbol{\tau_i} = C_Q\Omega_i^2\tilde{k}^{r_i} \quad (20)$$

A more detailed analysis for the thrust and the drag moment model is given in (Eq. 21) and (Eq. 22) where air density $\rho$ is captured separately,[11,13] allowing the model to be more accurate for changing environmental conditions.

$$\boldsymbol{f_i} = \rho A R^2 C_T\Omega_i^2\tilde{k}^{r_i} \quad (21)$$

$$\boldsymbol{\tau_i} = \rho A R^2 C_Q\Omega_i^2\tilde{k}^{r_i} \quad (22)$$

Although the model for thrust and moment in (Eq. 21) and (Eq. 22) seems to capture more physics compared to the much simpler models, it still lacks few physical phenomena that makes it less accurate relative to the higher order models in (Eq. 23) and (Eq. 24). The terms $C_T$ (thrust coefficient) and $C_Q$ (moment coefficient) are considered constants in literature, where in reality, the rotors' produced thrust also changes with the air inflow entering rotor's disk. Furthermore, the airflow due to the motion and the different tilt angles of each rotor causes each propeller to produce different thrust at the same angular velocity. This results in undesirable moments on the frame during side motion.[16]

In literature, momentum theory is used to study the thrust produced by the rotor.[15] The definition in Eq. 23 and Eq. 24 uses the US customary definition, which introduces a fraction of half.

$$f_i = \frac{1}{2}\rho A\Omega_i^2 R^2 C_T\tilde{k}^{r_i} \quad (23)$$

$$\tau_i = \frac{1}{2}\rho A\Omega_i^2 R^3 C_Q\tilde{k}^{r_i} \quad (24)$$

The thrust coefficient can be modelled as in Eq. 25:

$$C_{T_i} = \frac{1}{2}\sigma C_{l_\alpha}\left(\frac{\theta_0}{3} + \frac{\theta_{tw}}{4} - \frac{\lambda_i}{2}\right) \quad (25)$$

, where $\sigma$ is the rotors' solidity scalar, $C_{l_\alpha}$ is the lift coefficient of the rotor airfoil, $\theta_0$ is the rotor pitch angle at the root, $\theta_{tw}$ is the rotor twist, and $\lambda_i$ is the rotors' inflow ratio. The rotor pitch angle $\theta_0$ is considered as constant in case of tilt-quadrotor, while this variable can be as system input for platforms with variable pitch rotors. This model assumes the twist of the rotor to be linear, and also assumes the inflow on the rotor is uniform across the blade length. This model is studied from in details from momentum theory by Leishman.[15]

The rotor solidity $\sigma$ is the ration of the lifting area of the blades to the area of the rotor. This factor can be obtained using:

$$\sigma = \frac{N_b c}{\pi R} \quad (26)$$

, where $N_b$ is the number of blades, and $c$ is the blade chord length.

The induced inflow ratio $\lambda$ depends on induced inflow velocity $v_i$, climb rate $V_z$, and rotor tip speed $\Omega R$. The induced inflow ration is modelled as:

$$\lambda_i = \frac{V_z + v_i}{R\Omega_i} \quad (27)$$

The inflow velocity $v_i$ model is complex compared to the rest of the system. The model is divided into three definition in literature, where each definition is valid within a certain region (see Eq. 28). The inflow velocity $v_i$ is modelled as:

$$v_i = \begin{cases} -\frac{1}{2}V_z + \sqrt{\frac{1}{4}V_z^2 + v_h^2} & V_z \geq 0 \\ v_h\kappa + v_h\sum_{i=1}^{4} k_i\left(\frac{V_z}{v_h}\right)^i & -2 \leq \frac{V_z}{v_h} < 0 \\ -\frac{1}{2}V_z - \sqrt{\frac{1}{4}V_z^2 + v_h^2} & \frac{V_z}{v_h} < -2 \end{cases} \quad (28)$$

, where $v_h$ is the induced inflow velocity at hover, and is defined as:

$$v_h = \sqrt{\frac{T_h}{2\rho A}} \quad (29)$$

, where $T_h$ is the rotor thrust required for hover.

When the system is at hover or climbing ($V_z \geq 0$), the first definition of $v_i$ is used. However, the model of $v_i$ during descend is divided into two definitions according to the descend velocity. When the descend velocity is less than twice the hover inflow velocity, the slipstream produced by the rotor can be upward or downward of the rotor. This resulted in a more complicated model for the region $-2 \leq \frac{V_z}{v_h} < 0$. When the descend velocity is relatively high ($\frac{V_z}{v_h} < -2$), the slipstream is above the rotor, and is modelled as in third definition in Eq. 28.

The climb rate $V_z$ is the total inflow due to motion and wind.

$$\begin{bmatrix} V_x \\ V_y \\ V_z \end{bmatrix} = R^{br_i} \times \begin{bmatrix} u_r \\ v_r \\ w_r \end{bmatrix}^b = R^{br_i} \times \left( \begin{bmatrix} u \\ v \\ w \end{bmatrix}^b + R^{wb} \times (\boldsymbol{W^w} + \boldsymbol{W^r}) \right) \quad (30)$$

The model for $\boldsymbol{W^r}$ consists of induced airflow from individual rotors onto the environment, as well as rotor-to-rotor airflow interaction. This model is investigated experimentally for conventional quadrotors,[46] while there is still a gap for tilt-quadrotors.

The model in (Eq.30) can be extended further to include the induced airflow from the adjacent rotors.

## *Control System*

The control system is designed in literature mainly using either: Feedback Linearisation, or Control Allocator. Other control techniques for tilt-quadrotors are also studied, such as back-stepping and nonlinear $H_\infty$.[43,44]

*Feedback Linearisation* The main concept in Feedback Linearisation type controllers is to derive a control law, such that the closed-loop is a linear system. The selection of the controller depends on the structure of the nonlinear system to be controlled. This technique was studied for conventional quadrotor and tilt-quadrotor.[9,45]

The stabilisation and control of the tilt-quadrotor using Feedback Linearisation technique is studied by R. Markus and A. Saif.[9,45] The outcome of the study[9] was carried over for experimental study and further research.[8,18] The research assumed that the transient response of tilting motor is very fast, and also neglected the internal gyroscopic effects. With these assumptions, the tilting and gyroscopic effect dynamics were ignored in the control design.

The study by Markus presented a static feedback linearisation controller,[9] and concluded that this controller is not feasible for real time implementation. An alternative approach is a dynamic feedback linearisation which is based on the nonlinear model (refer to the original paper for detailed model of (Eq. 31)):

$$\begin{bmatrix} \ddot{\boldsymbol{P}} \\ \ddot{\boldsymbol{\omega}}_{\boldsymbol{B}} \end{bmatrix} = \boldsymbol{A}(\boldsymbol{\alpha}, \boldsymbol{w}) \begin{bmatrix} \dot{\boldsymbol{w}} \\ \boldsymbol{w}_{\boldsymbol{\alpha}} \end{bmatrix} + \boldsymbol{b}(\boldsymbol{\alpha}, \boldsymbol{w}, \boldsymbol{\omega_B}) \quad (31)$$

Using this nonlinear system model, the linearizing control law is:

$$\begin{bmatrix} \boldsymbol{w} \\ \boldsymbol{w}_{\boldsymbol{\alpha}} \end{bmatrix} = \boldsymbol{A}^+ \left( \begin{bmatrix} \ddot{\boldsymbol{p}}_{\boldsymbol{r}} \\ \ddot{\boldsymbol{\omega}}_{\boldsymbol{r}} \end{bmatrix} - \boldsymbol{b} \right) + (\boldsymbol{I_8} - \boldsymbol{A}^+\boldsymbol{A})\boldsymbol{z} \quad (32)$$

With the controller shown in (Eq. 32), the solution is feasible and overcomes the problem in the case of the static variant of the controller.

The final control scheme was tested in simulation. The simulation results showed that the control scheme is capable of tracking desired position and orientation independently (full 6-DoF control), and robust against neglected dynamics.[9]

*Control Allocation* The Control Allocation technique is one of the common methods to handle stabilisation and control of coupled systems. The general concept is to transform the nonlinear coupled system to decoupled subsystems then designing SISO controllers. This method offers the advantage of a modular design, where the high-level motion control algorithm can be designed without detailed knowledge about the actuators. The SISO controllers' output is fed into an allocator which couples all SISO controllers' outputs to the original coupled nonlinear system. This method was used in literature by several studies.[10–13] The diagram in Figure 7 gives a general structure for this type of controllers. This technique provides an abstract interface to control nonlinear systems, which allows classical SISO controllers to be designed and implemented. Furthermore, handling faults and failures does not usually require redesigning the controllers, only reconfiguration of the allocator is needed. On the other hand, this control technique has a disadvantages where it requires inverting the actuation model of the system.

**Figure 7.** General diagram of Control Allocator for coupled systems

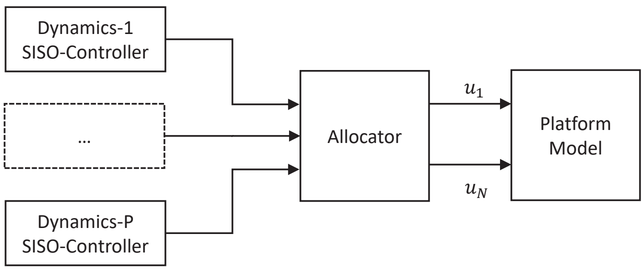


Designing the control system using the allocator approach was studied in literature to implement Stability Augmentation Control System for attitude control (SACS).[11] The controllers were classical PD, with the control allocator. This approach was chosen due to its simplicity and ease controller tuning.

Another work focused on studying and designing a control system capable of transitioning between normal system orientation ($\phi$, $\theta = 0°$) to perpendicular orientation ($\theta = 90°$).[10] The study resulted in two allocator controllers, each of which handles a different orientation.

The two allocator designs developed were validated and shown to work properly in simulation and experimentation.[10,11] The two-allocator approach is much simpler to implement compared to the single-allocator. However, the two-allocator approach is very specific to the orientations it was designed for, and has less operational range. While the single-allocator is a more generic design that works for all orientations. Furthermore, the two-allocator design might be less efficient, and difficult to reconfigure for fault cases, unlike the single-allocator design.

Although the term *Allocator* is not always used explicitly in literature, some of the work still apply the same conceptual design in the system. A valid approach to simplify designing of the allocator is to introduce constraints (all motors tilt with the same angle) in order to simplify the derivation of the inverse actuation.[19] This approach was used in literature to design an adaptive controller.[20]

## Recovery Strategy

### Overview

In order to propose a recovery strategy for tilt-quadrotors, two stages must be defined. These are Fault Detection and Isolation (FDI), and Fault Tolerant Control (FTC). In the FDI stage, the fault in the system is distinguished from external disturbances and nominal system behaviour. The second stage (FTC) is related to controlling the system in the presence of a pre-defined fault/failure case.

It is also important to distinguish in terminology between *Fault* and *Failure*. *Fault* is defined as 'an unpermitted deviation of at least one characteristic property (feature) of the system from the acceptable, usual, standard condition',[21,22] for example, undesired bias in sensor measurement from real value, or an actuator not capable of maintaining nominal command. While *Failure* is 'a permanent interruption of a systems ability to perform a required function under specified operating conditions', such as, a total loss of sensor measurement, or broken rotor (actuator). The presence of faults sometimes can lead to failures in the system if not detected or acted on remedy.

In the industry, a proper system analysis is performed by listing all possible failures and faults, their consequences, severity level, and probability of occurrence. Sets of failures and faults are categorised, and the focus is a set of failures and faults that has the worst combination of consequences, severity level and probability. Usually, actuators and sensors have the most catastrophic combination.

The recovery strategy is driven by a set of chosen objectives. The objectives can be as follows:

1. Completing mission regardless of faults and failures
2. Flying toward a predefined recovery trajectory
3. Maintaining flight efficiency
4. Capability of safe landing

Completing the mission is more suitable for military application. While the second objective is more suitable for civilian application. As an example, a network of drones for urban package delivery would prefer meeting objective-(2), and makes available a set of safe-landing points. While objective- (1), it might be impossible to have safe landing points and the mission needs to be carried out.

### Fault Detection and Isolation (FDI)

FDI is the task of 'inferring the occurrence of faults in a process and finding their root causes'.[23] There are various knowledge based strategies to design FDI, such as; quantitative models, qualitative models, and historical data. FDIs are two types, passive and active. An active FDI continuously excites the system and assesses the status by observing the system response. A passive FDI detects failures when the system severely suffers from a failure.

An FDI can be designed for detecting actuator faults in presence of environmental disturbances.[24] This problem can be handled by a strategy based on Nonlinear Geometric approach over two steps. In the first step, the Nonlinear Geometric approach is applied, and in the second step, a wind estimator is applied. The wind estimator consists of four estimators that are based on sliding mode technique.

The estimators provide estimation of wind and can also be affected by faults. Therefore, a procedure is defined to isolate faults from wind estimations.

The fault detection process in this case produces a set of residuals as output in a way that each fault '$\boldsymbol{f_i}$' affects different subset of residuals.[24] The module implemented for fault detection was tested in simulation. Sine wave with variable magnitudes and sweep of frequencies was used as wind function. A fault was injected to the simulation in presence of wind, results illustrated the impact of the fault on the residuals produced by the detection algorithm.

Another fault detection technique is possible through analysing vibration signals.[25] This is achieved by performing a three-level wavelet packet decomposition, resulting in eight wavelet component signals. The energy of the component signals is used as the feature vector to detect the faults. The detector (or *Diagnoser* as named by Jiang[25]) is a feedforward Artificial Neural Network (ANN). The ANN has three layers, an input layer, a hidden layer, and an output layer. The network is trained using vibration data from experiments. This data was preprocessed, and the features were extracted and fed to the ANN back propagation training algorithm. The datasets consists of faulty rotors such as; fractured blade, distorted blade, as well as healthy rotors. The results presented for the ANN detector showed correct detection and identification of faults with 98.2% success rate.

A variation of such detection techniques can use ANN with neurons replaced by fuzzy membership functions. This variation was used in literature to detect faults in navigation sensors, where a Gaussian membership function was used.[26] The training of the system can be carrier over offline using real sensors data. Although the interest of this review is the actuation failure, this approach can be applied by considering the actuation model instead of the navigation model.

Another technique to detect and isolate faults is to use detection filters.[27] The proposed approach produces decoupled detection spaces, where each space corresponds to certain actuator fault. The advantage of such approach is that it can handle different types of fault signals without adjusting the parameters of the detector. The detection filters defines observability matrix (detection space) for each fault. The detection space dimension is determined from the observability matrix.

There are five detection filters developed in literature.[27] Simulation results are presented for two cases: one for concurrent faults in two different actuators with designed decoupling filter, and the another for the same fault but without decoupling filter. The decoupling filter was shown to be very effective in isolating the fault of the actuators.

Another type of fault detection is based on Kalman Filters (KF).[28] The KF can be used for both; fault detection, and state estimation. The fault in this case is modelled as a percentage of effectiveness, ranging from normal status, to total loss of effectiveness (actuator failure). The final system model including the fault model is given in (Eq. 33), where $f_l$ is the effectiveness fault vector, and $F$ is the fault impact on system dynamics. The model in (Eq. 33) was used to derive the KF equations (including fault model), and these are;

propagation equation, and measurement update equation. A fault is declared according to the error residue between the output of the designed KF and system measurement. When the error residue exceeds a defined threshold, a fault is triggered by the detector. The study performed by Yu[28] presents a simulation results for a case where the KF has correctly declared an error, however, the work didn't clearly present how to distinguish between different faults.

$$\dot{\boldsymbol{x}} = \boldsymbol{A}\boldsymbol{x} + \boldsymbol{B}\boldsymbol{u} + \boldsymbol{F}\boldsymbol{f}_l \tag{33}$$

A recent research used adaptive Thau observer to detect faults and failures, and determine the severity level of the fault.[29]

## Fault Tolerant Control (FTC)

Fault Tolerant Control (FTC) is a branch of control system that is 'capable of controlling the system with satisfactory performance even if one or several faults, or more critically, one or several failures occur'.[21] A tailored version of this definition is suggested as: 'Control System capable of controlling the system to meet a set of defined objectives even if one or several faults, or more critically, one or several failures occur'.

Faults and failures in systems can be handled by two groups of methods, namely; *passive methods*, or *active methods*. A passive method ensures the capability of the system to handle faults through the design of robust controller that is capable of meeting certain performance measures in presence of faults or failures. An active method explicitly designs for the fault or failure, and acts accordingly once the fault or failure has been detected by the FDI.

FTC has different types, some of these types are; Multiple Model Techniques, Control Allocation Techniques, and Model Reference Adaptive Control. The Multiple Model Techniques have two types (sub-types), one is Multiple Model Switching and Tuning (MMST), and the other sub-type is Multiple Model Adaptive Estimation (MMAE), shown in Figure 8.

The Multiple Model techniques consists of, as the name suggests, several models to handle faults. The MMST technique is based on several separated dynamics models, each corresponds to an individual fault or failure. A specific controller is designed for each dynamics model. The system is reconfigured in a way to utilise an appropriate controller in presence of fault or failure. Similarly, the MMAE approach is based on a set of Kalman Filters (KF) that run in parallel, where each KF matches a particular failure case. The output of each KF goes through conditional probability calculation to determine the probability of each KF. The MMAE approach however is computationally expensive for embedded systems.

Another common technique for FTC is the Control Allocation Technique. This technique drives the control system design to produce a set of virtual commands (desired moments in this case). The virtual commands get processed to produce actuation commands using pseudo-inverse of the system actuation. The module is responsible for producing actuator commands from simulation, usually named *Control Allocator* in the literature. The Control Allocator takes into account the limitation of actuation in nominal faultless cases.

**Figure 8.** Multiple Model Adaptive Estimation technique[21]

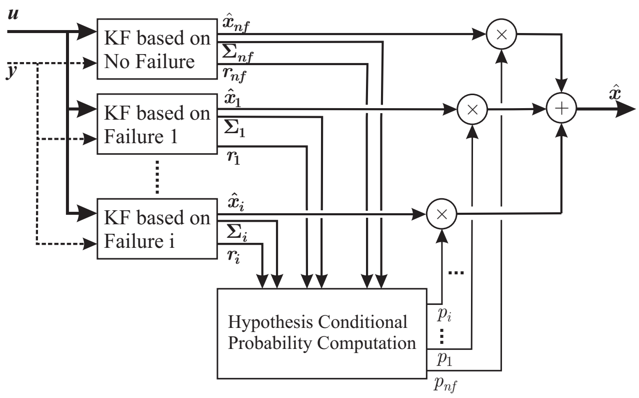


**Table 2.** Types of actuator faults and failures (extended to the list in literature).[21]

| | Cases | Description |
|---|---|---|
| 1 | Degraded | Actuator position not precisely at command |
| 2 | Bias | Actuator actual position is shifted from command |
| 3 | Stuck-at | Actuator position is stuck/fixed at certain output |
| 4 | Range-Limit | Actuator position range is lower than the usual range |
| 5 | Floating | Actuator position is floating and not following command |
| 6 | Hard-over | Actuator position is at maximum (or minimum) position |

For FTC purpose, the control allocator can be expanded to be configurable to handle fault cases as well as failure cases. The actuator failure can be handled using this approach without the need to changes the flight control laws. However, the drawback is that the control laws attempt to maintain the designed performance in presence of failure, regardless of the feasibility of virtual commands in the allocator.

Recent work in fault tolerant control in case of motor failure is performed by Nemati.[30] The study considered a single tilt-quadrotor with failure in a single rotor. For this case, a dynamic model was obtained for the moments and forces. The suggested strategy was to use the tilt angle of the rotor opposing the failed rotor, to compensate for the imbalance in the moments. While this approach shown to work in simulation, it is of great value to study the approach from practical point of view and how the reliability of the system is affected.

## Faults and Failures

Table 2 gives a list of defined faults and failures in the actuation of tilt-quadrotor. Although sensors are not covered, a list of possible faults and failures is given in Table 3.

The cases (1, 2, 3, 4) from Table 2 are considered faults, as the actuation is not totally lost. While the cases (5, 6) are considered failures. Real examples of case-1 are fractured blades and deformed blades (due to heat). For case-2 (Bias), this could happen if the actuation system is not calibrated.

**Table 3.** Types of sensor faults and failures[21]

| | Type | Description |
|---|---|---|
| 1 | Bias | Measurement corresponds to real value with a shift |
| 2 | Calibration | Measurement corresponds to scaled real value |
| 3 | Drift | Measurement drifts further from real value over time |
| 4 | Frozen | Measurement is stuck at fixed value regardless of real value |

Case-3 occurs when the electrical interface to the actuation is lost, in which the actuation defaults is pre-programmed in a failed safe position. A common example of case-4 (Range-Limit) is the degraded motors due to ageing or high accumulated running hours.

The last two cases are the failure cases. The Floating case is more common for fixed-wind aircraft, in which the mechanical linkage breaks. This could occur in tilt-quadrotors if the motor coils fails, or the driver circuit fails such that the motor is free to spin. A more relevant and interesting case (compared to Floating) is the total loss at maximum or minimum position (case-6). This could generally occur in multirotors if one of the propellers crashes into an object, or the motor fails.

Real examples (Table 3) of case-1 sensor fault occurs if the gyroscope is not calibrated, while case-3 occurs for sensors that deviate in output with temperature changes (especially gyroscopes). Case-2 is common in magnetometers when placed near components (motors) that influence earth magnetic field. Case-4 occurs in MEMS sensors in general when the internal structure of the sensor get damaged, causing the sensor to loose the sensing capability while still electrically functional.

Sensor faults are important class of faults that may affect UAV systems. Sensor faults can range from a complete failure of sensors to less severe faults where sensors can provide less accurate physical measurements. These faults were extensively addressed in literature with suggestions for different fault mitigation strategies. For example, researchers proposed a magnetic compass fault detection method for GPS/INS/magnetic compass integrated navigation systems.[48] In this approach, the faults were assumed to be caused by the hard iron and soft iron effects and the detection strategy usesd statistical approaches. Different designs of complementary filters were used to compensate for compass reading errors and IMU inaccuracies caused by gyro drift and accelerometer bias.[49–51] Unscented Kalman filter was suggested to achieve better results in mitigating issues associated with low accuracy sensors.[52]

## Discussion

The summary of the covered topics in each corresponding research area is shown in Table 4, the legend for the table is provided in Table 5. The field of tilt-quadrotor is still relatively new, therefore, some of the research activities are listed were conducted on conventional quadrotors.

**Table 4.** Literature summary and covered fields in each research study

| | Platform | | Control | | | | | | Modelling | | | |
|---|---|---|---|---|---|---|---|---|---|---|---|---|
| References | Number of Tilt Axes | Design | PID & Allocator | Feedback Linearisation | Geometry Control | $H_\infty$ | Back-stepping | Recovery | Rigid Body | Rotor Dynamics | Hub Forces | Identification |
| 6 | 2 | X | X | | | | | | X | | | |
| 11 | 2 | X | X | | | | | | X | A | | X |
| 12 | 2 | X | X | | | | | | X | A | | X |
| 13 | 2 | X | X | | | | | | X | A | | X |
| 19 | 2 | | X | | | | | | X | S | | |
| 20 | 2 | | X | | | | | | X | S | | |
| 31 | 2 | | X | | | | | | X | S | | |
| 32 | 2 | | X | | | | | | X | S | | |
| 33 | 2 | | X | | | | | | X | S | | |
| 34 | 2 | | | X | | | | | X | S | | |
| 45 | 2 | | | X | | | | | X | S | | |
| 44 | 2 | | | | | | X | | X | S | | |
| 7 | 1 | X | | | | | | | | | | |
| 8 | 1 | X | | X | | | | | X | S | | X |
| 9 | 1 | | | X | | | | | X | S | | |
| 10 | 1 | X | X | | | | | | X | S | | |
| 18 | 1 | | | X | | | | | X | S | X | |
| 30 | 1 | | X | | | | | X | X | S | | |
| 35 | 1 | | X | | | | | | X | S | | |
| 36 | 1 | | X | | | | | | X | S | | |
| 37 | 1 | X | X | | | | | | X | S | | |
| 38 | 1 | | | | | | | | X | S | | |
| 43 | 1 | | | | | X | | | X | S | | |
| 24 | 0 | | | | | | | X | X | A+ | | |
| 25 | 0 | | | | | | | X | | A | | |
| 27 | 0 | | | | | | | X | X | S | | |
| 28 | 0 | X | | | | | | X | X | S | | |
| 29 | 0 | | | | | | | X | X | S | | |
| 39 | 0 | | | | | | | X | X | S | | |
| 40 | * | | | | X | | | | X | | | |
| 42 | *** | | | X | | | | | X | S | | |
| 41 | ** | X | | | | | | | X | S | X | |

In the summary presented in Table 4, it is noted that most studies covered single tilt-quadrotors. Furthermore, there is no fault tolerant control study performed on tilt-quadrotors (except of Nemati[30] study). Also, there is very little analysis performed of the impact of faults and failures on system dynamics. The rotor model used is mostly the simple model (Eq. 19 and Eq. 20). Most of the studies focused on the two control techniques, which are; classical PID, and Feedback Linearisation.

## Conclusion

The state of the art research in tilt-quadrotor platforms is presented in this review paper. Development of recovery strategy for this platform has not been addressed extensively in the literature, it is open research problem. This is valid for both fault detection, and fault control.

Furthermore, the control in normal operation is reasonably studied and investigated, but still lacks trying other control approaches aside from the common Feedback Linearisation and Allocator techniques. A comparison between different

**Table 5.** Literature summary legend for Table 1

| | |
|---|---|
| X | Field is covered by indicated research |
| 0 | Conventional quadrotor |
| 1 | Single tilt-quadrotor |
| 2 | Dual tilt-quadrotor |
| * | Model is generic, and proposed approach is applicable to both single and dual tilt |
| ** | Not a quadrotor, rather a tiltrotor aircraft. Considered here since the model is very relevant |
| *** | Central dual tilt quadrotor, where all rotors have the same tilt angles |
| S | Simple rotor dynamics model - see models (Eq. 19) and (Eq. 20) |
| A | Advanced rotor dynamics model - see models (Eq. 21) and (Eq. 22) |
| A+ | More advanced rotor dynamics model |

control techniques in tracking difficult trajectories will allow better use of tilt-quadrotor platforms in urban and indoor applications.

Modelling tilt-quadrotors has been covered extensively with different level of complexity. Most of the dynamic model elements of conventional quadrotors are applicable to tilt-quadrotor platforms. However, there is a room for improving in the modelling side by considering surrounding airflow impact on system model, which will help in studying and understanding the system dynamics for indoor applications.

## References


1. Flight. Mention de l'hélicoptère d'Œhmichen 1921; : 160.
2. 740 FN. The de Bothezat Helicopter 1923; : 125.
3. Flight International Bell x-22a 1967; : 445–446.
4. Fluk H. The x-19 v/stol technology: A critical review. Technical report, CURTISS-WRIGHT CORP WOOD-RIDGE NJ WRIGHT AERONAUTICAL DIV, 1967.
5. Flight. CONVERTAWINGS, INC. 1956; : 722–723.
6. Junaid A, Sanchez A, Bosch J et al. Design and Implementation of a Dual-Axis Tilting Quadcopter. *Robotics* 2018; 7(4): 65. DOI:10.3390/robotics7040065.
7. Abde Quader, Alzu'bi HM, Abd Allateef I, Zweiri Y et al. Quad tilt rotor vertical take off and landing (vtol) unmanned aerial vehicle (uav) with 45 degree rotors, 2013. DOI: US20100322867A1. arXiv:1208.5721.
8. Ryll M, Bulthoff HH and Robuffo Giordano P. First Flight Tests for a Quadrotor UAV with Tilting Propellers. *IEEE Int Conf on Robotics and Automation* 2013; : 295–302DOI: 10.1109/ICRA.2013.6630591⟩.
9. Ryll M, Bulthoff HH and Giordano PR. Modeling and Control of a Quadrotor UAV with Tilting Propellers. *IEEE Int Conf on Robotics and Automation* 2012; : 4606–4613DOI:10.1109/ICRA.2012.6225129.
10. Oosedo A, Abiko S, Narasaki S et al. Flight control systems of a quad tilt rotor unmanned aerial vehicle for a large attitude change. In *IEEE International Conference on Robotics and Automation (ICRA), 2015*. IEEE, pp. 2326–2331. DOI:10.1109/ICRA.2015.7139508.
11. Al-Rihani Y, Segui Gasco P, Shin HS et al. Modelling and simulation of a novel dual axes tilt quadrotor uav. In *AIAA Modeling and Simulation Technologies (MST) Conference*. p. 4595. DOI:10.2514/6.2013-4595.
12. Segui-Gasco P, Al-Rihani Y, Shin HS et al. A novel actuation concept for a multi rotor UAV. *Journal of Intelligent \& Robotic Systems* 2014; 74(1-2): 173–191. DOI:10.1007/s10846-013-9987-3.
13. Gasco PS. *Development of a Dual Axis Tilt Rotorcraft UAV: Modelling, Simulation and Control*. PhD Thesis, Cranfield University, 2012.
14. Beard RW and McLain TW. *Small unmanned aircraft: Theory and practice*. Princeton university press, 2012. ISBN 9780691149219.
15. Leishman GJ. *Principles of helicopter aerodynamics with CD extra*. Cambridge university press, 2006.
16. Diogenes HB and dos Santos DA. Modelling, design and simulation of a quadrotor with tilting rotors actuated by a memory shape wire. In *Congresso Brasileiro de Engenharia Mecnica (CONEM), August 2016*. DOI:10.20906/CPS/CON-2016-0452.
17. Selig M. Modeling propeller aerodynamics and slipstream effects on small uavs in realtime. In *AIAA Atmospheric Flight Mechanics Conference*. p. 7938.
18. Ryll M, Bulthoff HH and Robuffo Giordano P. A Novel Overactuated Quadrotor UAV: Modeling, Control and Experimental Validation. *IEEE Transactions on Control Systems Technology* 2015; 23(2): 540–556. DOI:Doi10.1109/Tcst.2014.2330999.
19. Senkul F and Altug E. Modeling and Control of a Novel Tilt Roll Rotor Quadrotor UAV. *International Conference on Unmanned Aircraft Systems (ICUAS)* 2013; : 1071–1076.
20. Senkul F and Altug E. Adaptive Control of a Tilt Roll Rotor Quadrotor UAV.pdf. *International Conference on Unmanned Aircraft Systems (ICUAS)* 2014; : 1132–1137.
21. Ducard GJJ. *Fault-Tolerant Flight Control and Guidance Systems for a Small Unmanned Aerial Vehicle*. PhD Thesis, ETH ZURICH, 2007.
22. Isermann R. *Fault-Diagnosis Systems: An Introduction from Fault Detection to Fault Tolerance*. Springer, 2006. ISBN 3-540-24112-4.
23. Noura H, Theilliol D, Ponsart J et al. *Fault-Tolerant Control Systems: Design and Practical Applications*. Springer, 2009. ISBN 978-1-84882-652-6.
24. Castaldi P, Mimmo N, Naldi R et al. Robust Quadrotor Actuator Fault Detection and Isolation in Presence of Environmental Disturbances. *2016 European Control Conference, ECC 2016* 2017; : 1892–1897DOI:10.1109/ECC.2016.7810567.
25. Yan J, Zhao Z, Liu H et al. Fault Detection and Identification for Quadrotor Based on Airframe Vibration Signals: A Data-Driven Method. *Chinese Control Conference, CCC* 2015; 2015-Septe: 6356–6361. DOI:10.1109/ChiCC.2015.7260639.
26. Zhang Q, Wang X, Xiao X et al. Design of a fault detection and diagnose system for intelligent unmanned aerial vehicle navigation system. *Proceedings of the Institution of Mechanical Engineers, Part C: Journal of Mechanical Engineering Science* 2018; DOI:10.1177/0954406218780508.
27. Herdjunanto S. Actuator Fault Signal Isolation of an Unmanned Aerial Vehicle (UAV) Quadrotor Based on Detection Filter. *8th International Conference on Information*

*Technology and Electrical Engineering (ICITEE)* 2016; (3). DOI:10.1109/ICITEED.2016.7863232.

28. Yu B, Zhang Y, Yi Y et al. Fault Detection for Partial Loss of Effectiveness Faults of Actuators in a Quadrotor Unmanned Helicopter. *Proceedings of the World Congress on Intelligent Control and Automation (WCICA)* 2015; 2015-March(March): 3204–3209. DOI:10.1109/WCICA.2014.7053244.
29. Cen Z, Noura H and Younes YA. Systematic Fault Tolerant Control Based on Adaptive Thau Observer Estimation for Quadrotor Uavs. *International Journal of Applied Mathematics and Computer Science* 2015; 25(1): 159–174. DOI:10.1515/amcs-2015-0012.
30. Nemati A, Kumar R and Kumar M. Stabilizing and Control of Tilting-Rotor Quadcopter in Case of a Propeller Failure. In *ASME 2016 Dynamic Systems and Control Conference*. October, ASME. ISBN 978-0-7918-5069-5. DOI:10.1115/DSCC2016-9897.
31. Elfeky M, Elshafei M, Saif AWA et al. Quadrotor helicopter with tilting rotors: Modeling and simulation. In *2013 World Congress on Computer and Information Technology (WCCIT)*. Sousse, Tunisia: IEEE. ISBN 978-1-4799-0460-0, pp. 1–5. DOI:10.1109/WCCIT.2013.6618768.
32. Elfeky M, Elshafei M, Saif AWA et al. Quadrotor with tiltable rotors for manned applications. *2014 IEEE 11th International Multi-Conference on Systems, Signals & Devices (SSD14)* 2014; : 1–5DOI:10.1109/SSD.2014.6808791.
33. Aliyu A, Elshafei M, Saif AWA et al. Performance evaluation of quadrotor with tilted rotors under wind gusts. *IEEE/ASME International Conference on Advanced Intelligent Mechatronics, AIM* 2016; : 294–299DOI:10.1109/AIM.2016.7576782.
34. Rajappa S, Ryll M, Bulthoff HH et al. Modeling, control and design optimization for a fully-actuated hexarotor aerial vehicle with tilted propellers. In *2015 IEEE International Conference on Robotics and Automation (ICRA)*. IEEE. ISBN 978-1-4799-6923-4, pp. 4006–4013. DOI:10.1109/ICRA.2015.7139759.
35. Nemati A and Kumar MM. Modeling and control of a single axis tilting quadcopter. In *American Control Conference (ACC), 2014*. IEEE. ISBN 978-1-4799-3272-6, pp. 3077–3082. DOI:10.1109/ACC.2014.6859328.
36. Badr S, Mehrez O and Kabeel AE. A novel modification for a quadrotor design. *2016 International Conference on Unmanned Aircraft Systems, ICUAS 2016* 2016; : 702–710DOI:10.1109/ICUAS.2016.7502536.
37. Arakawa A, Hasegawa T, Watanabe K et al. Control of Attitude Angle for a Tilted Quadrotor. *2018 IEEE International Conference on Mechatronics and Automation (ICMA)* 2018; : 1844–1849DOI:10.1109/ICMA.2018.8484436.
38. Lin F, Zhang Y, Lu Y et al. A new style tilt-quadrotor: Modeling and exploration of its dynamical characteristics. In *2017 36th Chinese Control Conference (CCC)*. IEEE. ISBN 978-988-15639-3-4, pp. 2259–2264. DOI:10.23919/ChiCC.2017.8027694.
39. Morozov YV. Emergency Control of a Quadrocopter in Case of Failure of Two Symmetric Propellers. *Automation and Remote Control* 2018; 79(3): 463–478. DOI:10.1134/S0005117918030062.
40. Franchi A, Carli R, Bicego D et al. Full-Pose Tracking Control for Aerial Robotic Systems With Laterally Bounded Input Force. *IEEE Transactions on Robotics* 2018; 34(2): 534–541. DOI:10.1109/TRO.2017.2786734. 1605.06645.
41. Kendoul F, Fantoni I and Lozano R. Modeling and control of a small autonomous aircraft having two tilting rotors. *Proceedings of the 44th IEEE Conference on Decision and Control, and the European Control Conference, CDC-ECC '05* 2006; 22(6): 1297 – 1302. DOI:10.1109/TRO.2006.882956.
42. Odelga M, Stegagno P and Bulthoff HH. A fully actuated quadrotor UAV with a propeller tilting mechanism: Modeling and control. In *2016 IEEE International Conference on Advanced Intelligent Mechatronics (AIM)*. IEEE. ISBN 978-1-5090-2065-2, pp. 306–311. DOI:10.1109/AIM.2016.7576784.
43. Raffo GV, Ortega MG and Rubio FR. Nonlinear $H_\infty$ controller for the quad-rotor helicopter with input coupling. *IFAC Proceedings Volumes* 2011; 44(1): 13834–13839.
44. Saif AWA, Aliyu A, Al Dhaifallah M et al. Decentralized backstepping control of a quadrotor with tilted-rotor under wind gusts. *International Journal of Control, Automation and Systems* 2018; 16(5): 2458–2472.
45. Saif AWA. Feedback linearisation control of quadrotor with tiltable rotors under wind gusts. *International Journal of Advanced and Applied Sciences* 2017; 4(10): 150–159.
46. Zhou W, Ning Z, Li H et al. An experimental investigation on rotor-to-rotor interactions of small uav propellers. In *35th AIAA Applied Aerodynamics Conference*. p. 3744.
47. DossM AN. Cogging torque reduction in brushless dc motor by shaping of rotor magnets and modifying stator slots. *PhD Thesis, SRM University* 2015; .
48. Park SG, Jeong HC, Kim JW et al. Magnetic compass fault detection method for gps/ins/magnetic compass integrated navigation systems. *International Journal of Control, Automation and Systems* 2011; 9(2): 276. DOI:10.1007/s12555-011-0209-0. URL https://doi.org/10.1007/s12555-011-0209-0.
49. Yun X, Bachmann ER, McGhee RB et al. Testing and evaluation of an integrated gps/ins system for small auv navigation. *IEEE Journal of Oceanic Engineering* 1999; 24(3): 396–404. DOI:10.1109/48.775301.
50. Euston M, Coote P, Mahony R et al. A complementary filter for attitude estimation of a fixed-wing uav. In *2008 IEEE/RSJ International Conference on Intelligent Robots and Systems*. pp. 340–345. DOI:10.1109/IROS.2008.4650766.
51. Pflimlin JM, Hamel T and Soures P. Nonlinear attitude and gyroscope's bias estimation for a vtol uav. *International Journal of Systems Science* 2007; 38(3): 197–210. DOI:10.1080/00207720601110798. URL https://doi.org/10.1080/00207720601110798. https://doi.org/10.1080/00207720601110798.
52. Zhang P, Gu J, Milios EE et al. Navigation with imu/gps/digital compass with unscented kalman filter. In *IEEE International Conference Mechatronics and Automation, 2005*, volume 3. pp. 1497–1502 Vol. 3. DOI:10.1109/ICMA.2005.1626777.